PHYSICAL REVIEW LETTERS

VOLUME 9 DECEMBER 15, 1962 NUMBER 12

COHERENCE STUDIES OF EMISSION FROM A PULSED RUBY LASER

David A. Berkley and George J. Wolga
Cornell University,* Ithaca, New York
(Received November 13, 1962)

The emission from a ruby laser typically consists of many intense pulses of about one-half-microsecond width each, the total emission lasting for several hundred microseconds. Adjacent pulses are rarely of equal intensity, are not strictly periodic in time, and the emission intensity often drops to a low value, perhaps zero, between pulses. It is important to measure the temporal and spatial coherence of this laser emission both to specify its character and to understand the underlying physical processes involved in laser action. Spatial coherence for the ruby laser over a distance of 0.0054 cm was demonstrated by Nelson and Collins[1] and over a distance of 0.32 cm by Hercher.[2] Both these experiments examined spatial coherence in the near field. To our knowledge temporal coherence of ruby-laser emission has not been experimentally studied. The infrared laser emission from the helium-neon gas laser was shown to be time coherent for at least 0.0041 μsec.[3] The theory of partially coherent light[4] specifies the coherence of a light source by the cross-correlation function that determines the visibility of the interference pattern obtained by superposing the radiation from two secondary sources. We wish to report a study of the cross-correlation function of the far-field ruby-laser emission, in which we obtained clear interference fringes from two slits that were separately illuminated by different parts of the laser-beam cross section and with a variable delay time τ between the illuminating of one slit and the subsequent illuminating of the other slit by a portion of the same wave front.

The apparatus we used is shown in Fig. 1. The laser cavity is a high-efficiency elliptic cylinder reflector[5] which contains a 3-inch long, $\frac{1}{4}$-inch diameter, 90° orientation, uncooled ruby with flat, silvered ends. One end was opaque while the other transmitted 5%. The laser was operated at an energy input to the lamp not more than 28 joules above the threshold value of 130 joules. The laser beam was split (wavefront division) by prism P_1, and the deflected portion sent through a distance l, totally reflected in prism P_2, partially focused by a cylinder lens, and finally reflected onto one slit. The other slit was directly illuminated by the undeflected portion of the beam. In our experiments at long delay lengths we decreased the divergence of the beam by passing the beam through a 5.5-power telescope used in reverse and focused at infinity prior to splitting the beam. Interference fringes were photographed on Polaroid Type 47 film used as a screen, for many delay lengths between 18 cm and 2520 cm. The width of the main lobe of the single-slit diffraction patterns and the separation of the fringes agree with calculations using the slit widths and slit separation indicated in Fig. 1. We could no longer see fringes on our photographs for $\Delta l = 3000$ cm, which leads us to limit the coherence length in these experiments to $2520 < \Delta l < 3000$ cm. It is clear that we depend on spatial coherence in the far laser field in this experiment, and since we have obtained

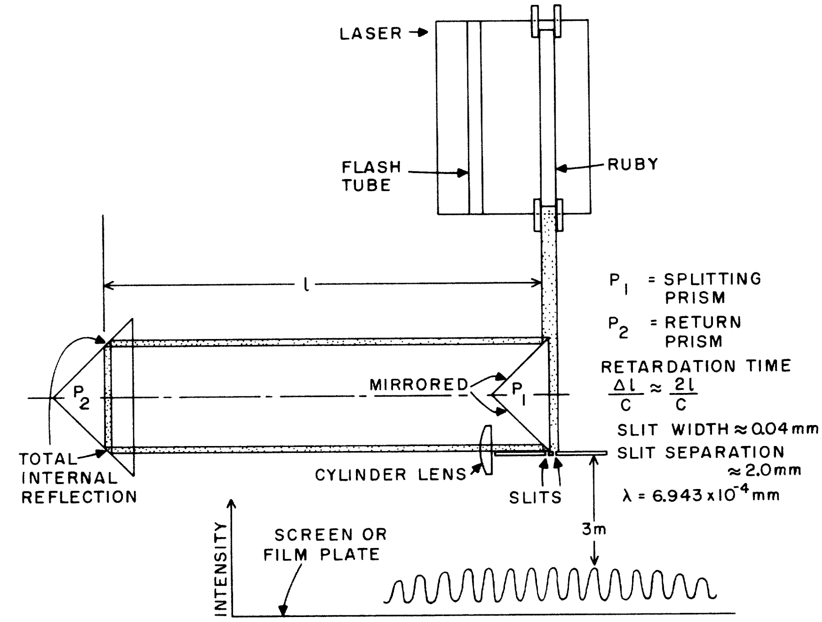

FIG. 1. Schematic diagram of the experiment.

interference fringes with slit separations of 0.405 cm we have thereby observed spatial coherence in the far field for such distances. Figure 2 shows microphotometer tracings over a portion of the interference pattern obtained in three separate experiments in which photographs were made on Kodak Royal-X-Pan film. Curve (*a*) shows fringes obtained by directly illuminating

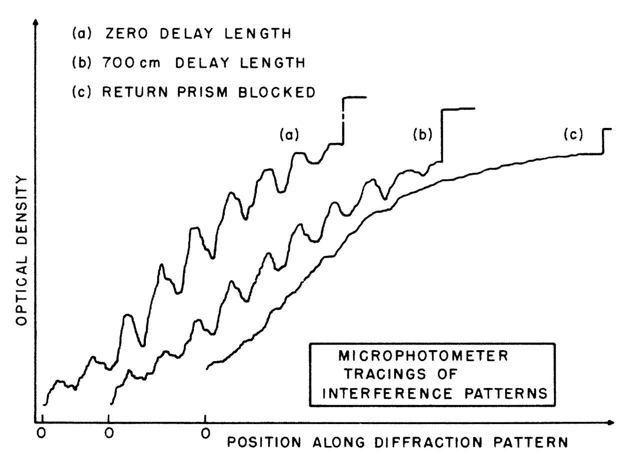

FIG. 2. Microphotometer traces of the photographed interference pattern for an entire ruby-leser emission period of several hundred microseconds. The slit widths and separation are identical to those described on Fig. 1. (*a*) Zero delay length; (*b*) 700-cm delay length; (*c*) return prism P_2 removed.

both slits. Curve (*b*) shows fringes for a delay length of 700 cm. Curve (*c*) shows a microphotometer trace for an experiment where prism P_2 was removed, thus preventing direct illumination of one of the slits. Since no fringes are visible we conclude that there is negligible light leakage from the directly illuminated slit to the other slit.

Our experiment indicates that fringe visibility defined by

$$V = \frac{\langle I_{\max}\rangle - \langle I_{\min}\rangle}{\langle I_{\max}\rangle + \langle I_{\min}\rangle}, \tag{1}$$

measured for adjacent fringes, decreases below the observable level (about 1 %) for $2502 < \Delta l < 3000$ cm. In an attempt to interpret this result we employed a model for a laser pulse and calculated the cross-correlation function $\gamma_{12}(\tau)$, with $\tau = \Delta l/c$, which determines the fringe visibility. We let the electric field of a single laser pulse be a Gaussian envelope in time enclosing a monochromatic sine wave whose frequency is a laser axial mode frequency for our ruby. The Gaussian amplitude corresponded reasonably well to the pulse shapes we observed with a photomultiplier tube, and we chose the time duration of the pulse to correspond to the average pulse duration as observed with the photomultiplier tube. We converted the observed intensity pulses to equivalent amplitude pulses and found an average pulse duration of

0.56 μsec. The monochromatic carrier is suggested by McMurtry's and Siegman's[6] results on "zero-beating" experiments with ruby-laser photo beats. With $E_K^{(1)}f_K^{(1)}(t)$ and $E_K^{(2)}f_K^{(2)}(t+\tau)$ representing the electric field pulses at slits (1) and (2) from the Kth mode, we can express the average intensity or film density at a point on our screen corresponding to a delay τ as

$$\begin{aligned}\langle I\rangle &= \langle[E_K^{(1)}f_K^{(1)}(t)+E_K^{(2)}f_K^{(2)}(t+\tau)]^2\rangle,\\ &= (E_K^{(1)})^2\langle[f_K^{(1)}(t)]^2\rangle+(E_K^{(2)})^2\langle[f_K^{(2)}(t+\tau)]^2\rangle\\ &\quad+2E_K^{(1)}E_K^{(2)}\langle f_K^{(1)}(t)f_K^{(2)}(t+\tau)\rangle, \qquad (2)\end{aligned}$$

where K specifies an axial mode frequency $f_K = \omega_K/2\pi$ and the angular brackets represent a time average over our observation time which may be as long as the total laser emission but could be the duration of a single pulse. We define

$$\Gamma_{11}(0)=\langle[f_K^{(1)}(t)]^2\rangle, \qquad (3)$$

and assume this to be equal to $\langle[f_K^{(2)}(t+\tau)]^2\rangle$. We define

$$\Gamma_{12}(\tau)=\langle f_K^{(1)}(t)f_K^{(2)}(t+\tau)\rangle, \qquad (4)$$

and obtain

$$\begin{aligned}\langle I\rangle &= [(E_K^{(1)})^2+(E_K^{(2)})^2]\Gamma_{11}(0)\\ &\quad\times\{1+2E_K^{(1)}E_K^{(2)}/[(E_K^{(1)})^2+(E_K^{(2)})^2]\gamma_{12}(\tau)\}, \qquad (5)\end{aligned}$$

where $\gamma_{12}(\tau)=\Gamma_{12}(\tau)/\Gamma_{11}(0)$. With $f_K(t)=(\cos\omega_K t)\times\exp[-\frac{1}{2}(t/t_1)^2]$, we obtain

$$\Gamma_{11}(0)=\tfrac{1}{2}\pi^{1/2}t_1,$$

$$\Gamma_{12}(\tau)=\tfrac{1}{2}\pi^{1/2}t_1\exp(-\tau^2/4t_1^2)\cos\omega_K\tau,$$

and

$$\gamma_{12}(\tau)=\exp(-\tau^2/4t_1^2)\cos\omega_K\tau. \qquad (6)$$

The fringe visibility for a single mode becomes

$$\begin{aligned}V_K &= \frac{2E_K^{(1)}E_K^{(2)}}{(E_K^{(1)})^2+(E_K^{(2)})^2}\exp\left(-\frac{\tau^2}{4t_1^2}\right)\\ &= \frac{2(\langle I_K^{(1)}\rangle\langle I_K^{(2)}\rangle)^{1/2}}{\langle I_K^{(1)}\rangle+\langle I_K^{(2)}\rangle}\exp\left(-\frac{\tau^2}{4t_1^2}\right), \qquad (7)\end{aligned}$$

where $\langle I_K^{(1)}\rangle$ and $\langle I_K^{(2)}\rangle$ are the intensities of mode K emerging from the slits. We measured $\langle\sum_K I_K^{(1)}\rangle$ and $\langle\sum_K I_K^{(2)}\rangle$ for a delay of about 20 cm to take account of intensity losses in the reflections at P_1 and P_2, and we assumed their ratio to be the same for $\langle I_K^{(1)}\rangle$ and $\langle I_K^{(2)}\rangle$. We estimated the loss in intensity of $\langle I_K^{(2)}\rangle$ for the long delays by measuring the beam divergence and assuming a loss of intensity inversely proportional to the increase in beam area due to divergence. Since imperfect spatial coherence would also decrease the fringe visibility, we measured the fringe visibility at zero delay length and assumed that spatial and temporal incoherence act independently so that we could apply the spatial coherence at zero delay time as a multiplicative factor to V_K. Taking all this into account, we find $V_K = 0.06\exp(-\tau^2/4t_1^2)$ for $\tau = 0.1$ μsec corresponding to $\Delta l = 3000$ cm. At this distance, and using $t_1 = 0.34$ μsec corresponding to our amplitude width of 0.56 μsec, we conclude that the fringes should be faint but still easily observable. To render the fringes essentially unobservable, i.e., $V_K \leq 0.01$, we require $\tau \geq 0.9$ μsec. Thus the vanishing of the fringes at $\Delta l = 3000$ cm is within an order of magnitude of the limiting delay we calculate with our model for a single mode.

We also considered the simultaneous presence of two different modes. We find the correlation between different modes to be negligibly small. The only change is the addition of $\frac{1}{2}\pi^{1/2}t_1\exp(-\tau^2/4t_1^2)\cos\omega_{K'}\tau$ to $\Gamma_{12}(\tau)$, where $\omega_{K'}$ is the angular frequency of the second mode, and we find that

$$\gamma_{12}(\tau)=\tfrac{1}{2}\exp(-\tau^2/4t_1^2)(\cos\omega_K\tau+\cos\omega_{K'}\tau). \qquad (8)$$

Thus the presence of two modes simultaneously will not significantly decrease the fringe visibility. One feature, however, of having two modes present is a repetitive change in the fringe visibility corresponding to $\cos\omega_K\tau$ and $\cos\omega_{K'}\tau$ becoming out of phase. This "moding effect" has been observed with the continuous helium-neon laser,[3] and we have seen indications of it in our experiments. However, it is not a likely mechanism for total loss of fringe visibility since this would require that the same two modes be simultaneously present in most of the several hundred pulses that are recorded during the total laser emission. Our experiments[7] on "moding effects" suggest that this is not the case as do McMurtry's and Siegman's[6] results.

The explanation of the premature loss in fringe visibility probably depends on some other physical process. One possibility is that since our photomultiplier response is not fast enough to record amplitude variations within the 0.56-μsec amplitude pulses, we could be missing some finer structure of these pulses. If t_1 was reduced by an order of magnitude, our model would predict a loss of fringe visibility as observed. Another possibility is that spatial coherence associated with two regions across the beam and separated by a time delay τ is degraded with increasing delay length.

We would like to acknowledge helpful conversations with Professor L. Wagner.

*This work was supported entirely by the Advanced Research Projects Agency.

[1]D. F. Nelson and R. J. Collins, J. Appl. Phys. 32, 739 (1961).

[2]Michael Hercher, Appl. Optics 1, 665 (1962).

[3]D. R. Herriot, Advances in Quantum Electronics, edited by J. R. Singer (Columbia University Press, New York, 1961).

[4]M. Born and E. Wolf, Principles of Optics (Pergamon Press, New York, 1959).

[5]B. W. Woodward and G. J. Wolga (to be published).

[6]B. J. McMurtry and A. E. Siegman, Appl. Optics 1, 51 (1961).

[7]Unpublished results.

OSCILLATORY MAGNETIC BREAKDOWN IN ZINC*

R. W. Stark
Physics Department, Case Institute of Technology, Cleveland, Ohio
(Received November 13, 1962)

Previous experimental data on the galvanomagnetic properties of zinc single crystals have shown that very large amplitude Shubnikov–de Haas oscillations are found for magnetic field directions near the c axis of this hexagonal close-packed metal.[1] These oscillations are associated with a very small, needle-shaped portion of the Fermi surface which contains approximately 10^{-6} of the conduction electrons in zinc. The amplitude of these oscillations appears to be many orders of magnitude larger than any existing theory would predict. We have found that these oscillations are not of the normal Shubnikov–de Haas type as previously thought, but are caused by a perturbation of magnetic breakdown by the position, relative to the Fermi energy, of the Landau levels of the needle-shaped portion of the Fermi surface. This magnetic breakdown produces a giant orbit like that previously found in magnesium.[2-4]

The de Haas–van Alphen measurements of Joseph and Gordon[5] and the magnetoacoustic measurements of Gibbons and Falicov[6] indicate that the Fermi surface of zinc is nearly identical to Harrison's single orthogonalized plane-wave model[7] as modified by Cohen and Falicov[8] to take into account the effects of spin-orbit coupling. The second band hole surface (the "monster") of this model is multiply connected and will support open trajectories parallel to the hexagonal axis.

A thorough investigation of the transverse magnetoresistance of several single-crystal specimens of zinc has been completed using magnetic field strengths as high as 23 000 gauss. The results of this investigation indicate that the topological features of the Fermi surface of zinc are identical to those of magnesium[4] with the exception that the Fermi surface of zinc is open parallel to the sixfold hexagonal axis. This openness was not observed in magnesium presumably because of magnetic breakdown of the spin-orbit energy gap which is much smaller in magnesium than in zinc.

Figure 1 is a stereographic projection in reciprocal space of those directions of H which were found to produce open trajectories in zinc. Directions of H are given by the coordinates θ, the angle between H and the polar axis $\vec{b}_3$, and ϕ, the angle between the plane of H and $\vec{b}_3$ and the plane of $\vec{b}_1$ and $\vec{b}_3$. The periphery of the stereogram corresponds to H in the basal plane. These directions of H produce open trajectories parallel to $\vec{b}_3$. The radial lines which emanate from the pole of the stereogram are directions of H which produce open trajectories parallel to the basal plane. These open trajectories are of the same type as those observed earlier in magnesium[4] and are produced by magnetic breakdown of the energy gap which separates the second band hole surface, the monster, and the needle portions of the third band electron surface. The longer radial lines are directions of H which produce the ee type open trajectories, while the shorter radial lines give rise to the ff open trajectories, both of which are shown in